New Physics Models
and CP Violation Experiments

Dennis Silverman
Department of Physics and Astronomy
University of California, Irvine
http://www.physics.uci.edu/∼silverma/

April 1-7, 1998, Tropical Workshop

1 Introduction

- To decide whether the B Factory is significantly testing the standard CKM model of CP violation, and to determine the “reach” of the B factory in ruling out “new physics” models, we need several alternate but full physical models for comparison.
- The flavor changing neutral current (FCNC) model resulting from extra weak iso-singlet down quarks, as in E_6 with one for each generation, has been very effective in causing new effects, but not being ruled out by present experiments.
- In this talk, the predictions are **extended to the full range** of angular experimental results.
- The constraints are updated for **new x_s bounds**, and for **new data on** R_b, the D0 bound on $K \to \mu\mu X$, and the **BNL results** on $K^+ \to \pi^+ \nu\bar{\nu}$.
- With Herng Tony Yao we also analyze the **Left-Right Symmetric Model (LRSM)**.

- Most recent published version: D. Silverman, Int. Journal of Modern Physics A11, 2253 (1996), hep-ph/9504387.
- Previous collaborators: Myron Bander, Michael Shin, Yossi Nir, Woon-Seng Choong, Tony Yao.

2 FCNC in Z^0 Couplings From Extra Iso-singlet Down Quarks

Mixing Angles in the 4×4 Mixing Matrix Have 6 Angles and 3 Phases.

$$
V = \begin{array}{c} \\ u \\ c \\ t \\ 4 \end{array}
\begin{array}{c}
\begin{array}{cccc} \quad d \quad & \quad s \quad & \quad b \quad & \quad D \quad \end{array} \\
\begin{pmatrix}
c_{34} & s_{12}c_{34} & s_{13}e^{-i\delta_{13}} & s_{14}e^{-i\delta_{14}} \\
-s_{12} & 1 & s_{23} & s_{24}e^{-i\delta_{24}} \\
(s_{12}s_{23} - s_{13}e^{i\delta_{13}}) & -s_{23} & 1 & s_{34} \\
V_{4d} & V_{4s} & V_{4b} & V_{44}
\end{pmatrix}
\end{array}
$$

$$
\begin{aligned}
V_{4d}^* &= -s_{14}e^{-i\delta_{14}} + s_{24}e^{-i\delta_{24}}s_{12} - s_{34}(s_{12}s_{23} - s_{13}e^{-i\delta_{13}}), \\
V_{4s}^* &= -s_{24}e^{-i\delta_{24}} - s_{14}e^{-i\delta_{14}}s_{12} + s_{34}(s_{23} + s_{12}s_{13}e^{-i\delta_{13}}), \\
V_{4b}^* &= -s_{34} - s_{24}e^{-i\delta_{24}}s_{23} - s_{14}e^{-i\delta_{14}}s_{13}e^{i\delta_{13}}.
\end{aligned}
$$

FCNC Amplitudes The FCNC are given by the mixings to the fourth down quark by

$$-U_{ij} \equiv V_{4i}^* V_{4j} \quad \text{for} \quad i \neq j.$$

The FCNC couplings of the down quarks to the Z are then given by:

$$\mathcal{L}_{FCNC}^Z = -\frac{e}{2\sin\theta_W \cos\theta_W} U_{ij}\bar{d}_{iL}\gamma^\mu d_{jL}Z_\mu.$$

There will be constraints on three FCNC amplitudes:

$$
\begin{aligned}
-U_{ds} &= V_{4d}^* V_{4s} \\
-U_{sb} &= V_{4s}^* V_{4b} \\
-U_{bd} &= V_{4b}^* V_{4d}
\end{aligned}
$$

Diagonal Neutral Current Decrease The diagonal neutral current couplings are reduced in strength by the amplitudes into the FCNC, becoming

$$\mathcal{L}_{NC}^Z = -\frac{e}{2\sin\theta_W \cos\theta_W} \sum_i (1 - |V_{4i}|^2)\bar{d}_{iL}\gamma^\mu d_{iL}Z_\mu.$$

3 $B_d - \bar{B}_d$ Mixing

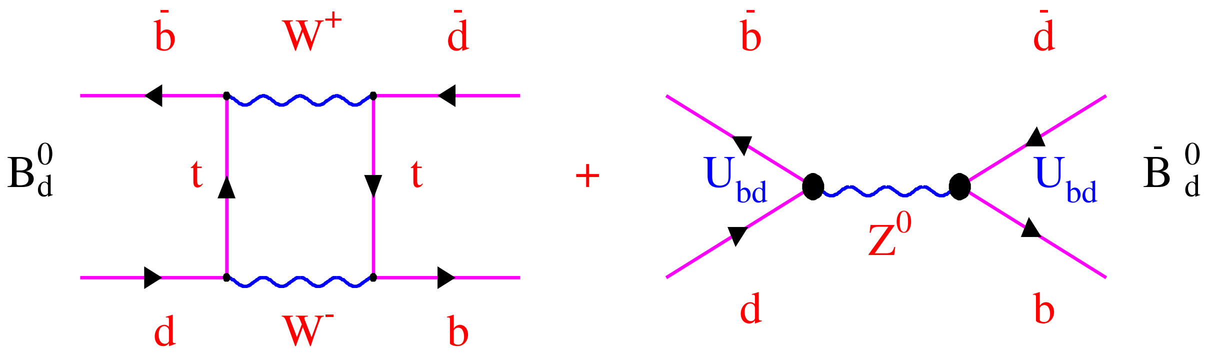

$$x_d = \frac{2G_F}{3\sqrt{2}} B_B f_B^2 m_B \eta_B \tau_B \left| U^2_{std-db} + (U_{db})^2 \right|$$

where $x_d = \Delta m_{B_d}/\Gamma_{B_d} = \tau_{B_d}\Delta m_{B_d} = \tau_{B_d} 2|M_{12}|$.

$$\begin{aligned} x_d &= 0.73 \pm 0.05, \\ \sqrt{B_B} f_B &= 0.200 \pm 0.040 \text{ GeV}. \end{aligned}$$

To leading order in s_{34}, $s_{24}e^{-i\delta_{24}}$, and $s_{14}e^{-i\delta_{14}}$ we have:

$$U_{db} = -s_{34}(s_{34}V^*_{td} + s_{14}e^{-i\delta_{14}} - s_{24}e^{-i\delta_{24}}s_{12}).$$

The first term has the phase δ_{13} as in the standard model, but the other two phases can also account for CP violation.

We define the standard model amplitude for $B_d - \bar{B}_d$ mixing from x_d normalized so that it adds directly to U^2_{db}

$$U^2_{std-db} \equiv \frac{\alpha}{4\pi \sin^2\theta_W} y_t f_2(y_t) (V^*_{td}V_{tb})^2.$$

4 Bounds on FCNC CP Violation in $|\epsilon|$

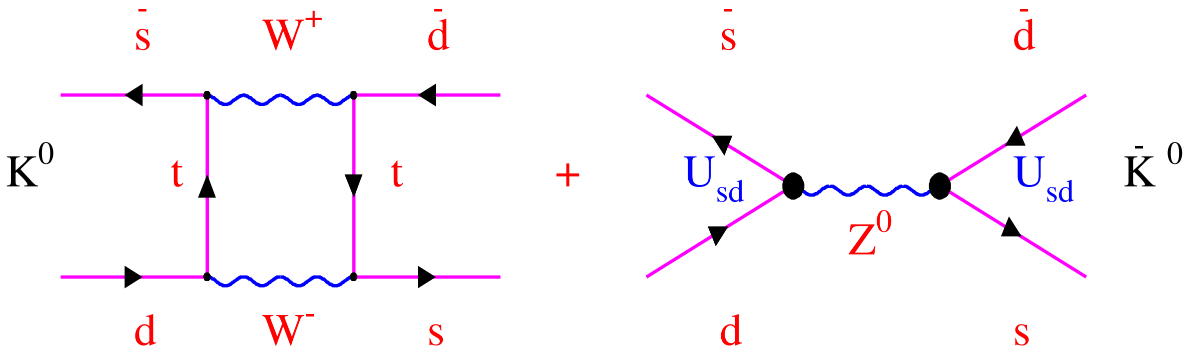

$$M_{12} =< K^0|H|\bar{K}^0 >$$

$$1 - 2\epsilon = \sqrt{\frac{M_{12}^*}{M_{12}}} \approx 1 - i\mathrm{Im}(M_{12})$$

$$|\epsilon| = 2.27 \times 10^{-3}$$

$$|\epsilon| = \frac{G_F f_K^2 B_K m_K}{12\Delta m_K} \left|\mathrm{Im}(U^2_{std-ds}) + \mathrm{Im}(U^2_{ds})\right|.$$

where

$$U^2_{std-ds} \equiv \frac{\alpha}{4\pi \sin^2\theta_W}(\eta_2 y_t f_2(y_t)(V_{td}^* V_{ts})^2 + \ldots)$$

$$\begin{aligned} |\mathrm{Im}[(U_{ds})^2]| &\leq 9.2 \times 10^{-10} \\ |\mathrm{Re}(U_{ds})\mathrm{Im}(U_{ds})| &\leq 4.6 \times 10^{-10} \end{aligned}$$

5 Bounds From $K^+ \to \pi^+\nu\bar{\nu}$

BNL E-787, analyzing their 1995 data, has now detected one event giving a branching ratio

$$\mathrm{BR}(K^+ \to \pi^+\nu\bar{\nu}) = 4.2^{+9.7}_{-3.5} \times 10^{-10}.$$

The standard model range is $(0.6 - 1.5) \times 10^{-10}$. The new result replaces their older bound of 2.4×10^{-9} at 90% CL.

The diagram on the right shows how the FCNC can contribute to this process. Diagrams for $s \to d + Z^0$ also exist in the standard model using penguins.

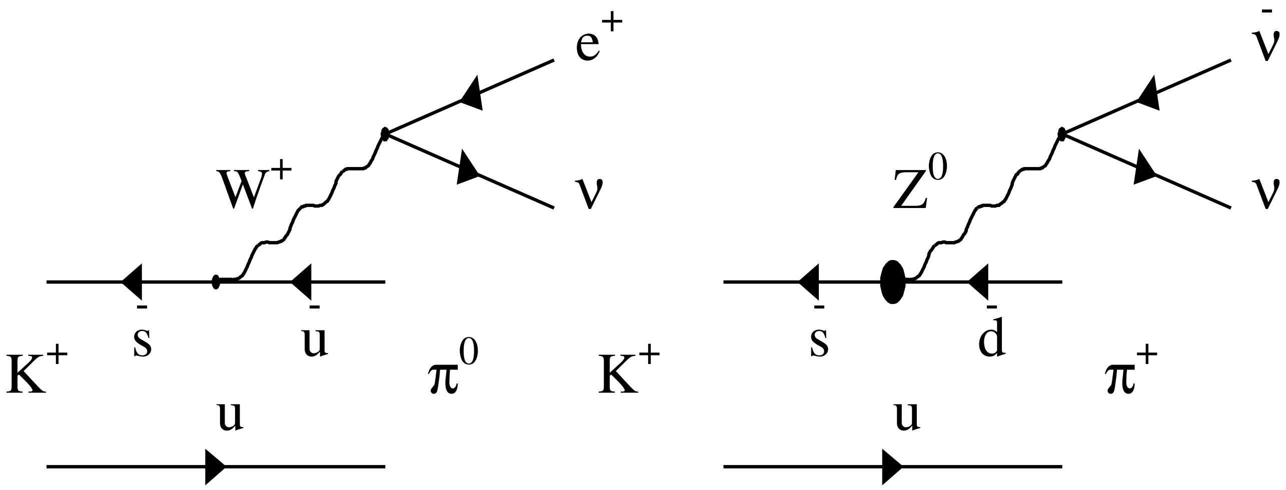

To cancel out the hadronic interactions, this is scaled to a ratio

$$\frac{\mathrm{BR}(K^+ \to \pi^+\nu\bar{\nu})}{\mathrm{BR}(K^+ \to \pi^0 e^+\nu)} = \frac{1}{2}\frac{|U_{ds}|^2}{|V_{us}|^2}.$$

This gives a contribution to $\chi^2 = 2 < n >= 2.4 \times 10^9\ |U_{ds}|^2$. The not very restrictive 1-σ limits on FCNC here are

$$6 \times 10^{-10} \leq |U_{ds}|^2 \leq 28 \times 10^{-10}.$$

6 Bound From $Z^0 \to b\bar{b}$

Weak isovector part of $Z^0 \to b\bar{b}$ reduced by $(1-|V_{4b}|^2)$

$$\begin{aligned}
V^b &= -\frac{1}{2}(1-|V_{4b}|^2) + \frac{2}{3}\sin^2\theta_W + \frac{1}{3}\rho_t, \\
A^b &= -\frac{1}{2}(1-|V_{4b}|^2) + \frac{1}{3}\rho_t \\
C_{QCD} &= 3(1.0385) \\
\Gamma^{std}(Z^0 \to b\bar{b}) &= \frac{C_{QCD} G_F m_Z^3}{6\sqrt{2}\pi}\left[(V^b)^2 + (A^b)^2\right]
\end{aligned}$$

where $\rho_t = 0.0094$ for $m_t = 174$ GeV. Present data and theory:

$$\begin{aligned}
R_b^{\text{Aleph(FiveTag)}} &= 0.2158 \pm 0.0014 \\
R_b^{\text{LEP+SLD}} &= 0.2170 \pm 0.0009 \\
R_b^{\text{theory}} &= 0.2158 \pm 0.0003 \\
\text{Difference} &= 0.0012 \pm 0.0009
\end{aligned}$$

Since the $|V_{4b}|$ effect is to decrease R_B, the conservative approach is to interpret the upward discrepancy as a fluctuation of statistical or systematic origin, and to still use the standard model result as the comparison point for setting the limit on $|V_{4b}|$. The experiment might be high due to another new effect, in which case we must still compare with the standard model. Also, in comparing with the SM in the CKM fits, no χ^2 contribution was entered from this experiment. With the above interpretation, the errors on the experiment are expanded to equal the deviation of 0.0012.

$$\frac{\Gamma_{b\bar{b}}^{std+FCNC}}{\Gamma_{b\bar{b}}^{std}} = (1 - 2.29|V_{4b}|^2)$$

$$\chi^2 = \left(\frac{0.2158 - 0.2158(1-2.29|V_{4b}|^2)}{0.0012}\right)^2.$$

7 CKM, FCNC, and B Factory Experiments

- **CKM Experiments (9) for Standard Model - Present Data**
  - **Charged Current (5):**
    V_{ud}, V_{us}, V_{cd}, and

$$
\begin{aligned}
|V_{cb}| &= 0.039 \pm 0.004 \\
|V_{ub}/V_{cb}| &= 0.080 \pm 0.020
\end{aligned}
$$

  - **Neutral Current (4):**

x_d	U_{db}
$\lvert\epsilon\rvert$	$\mathrm{Im}(U_{ds}^2)$
$K_L \to \mu\mu$	$\mathrm{Re}(U_{ds})$
x_s bound	U_{sb}

- **Exclusively FCNC Experiments for Four Down Quark Model (4)**

$B \to \mu\mu X$	UA1 and D0	$\lvert U_{db}\rvert$, $\lvert U_{sb}\rvert$
$Z^0 \to b\bar{b}$ (R_b)		$\lvert V_{4b}\rvert$
$K^+ \to \pi^+\nu\bar{\nu}$		$\lvert U_{ds}\rvert$

- **B Factory Projected Experiments (2)**

$\sin(2\beta)$	U_{db}^2
$\sin(2\alpha)$	U_{db}^2

8 CP Violating Asymmetries at the B Factory

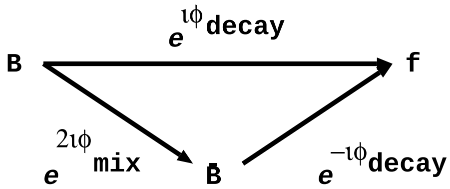

- $\sin(2\alpha)$ and $\sin(2\beta)$ are now defined as the measured B factory asymmetries, but they do not correspond to unitarity triangle or quadrangle angles in the four down quark model.

- $B_d^0 \to J/\Psi K_s^0$

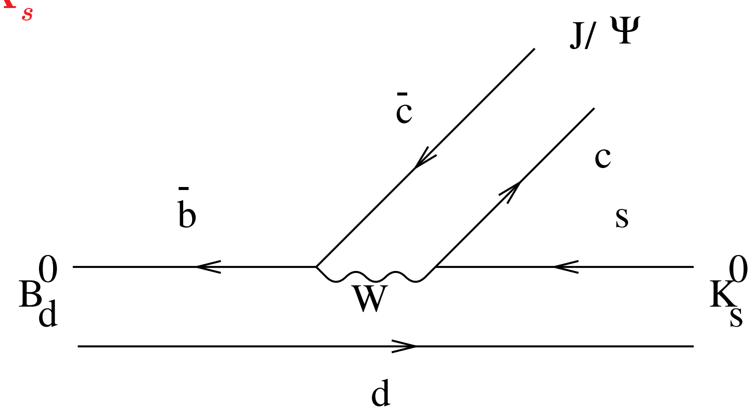

$$\sin(2\beta) \equiv A_{B_d^0 \to \Psi K_s^0} = \mathrm{Im}\left[\frac{(U_{std-db}^2 + U_{db}^2)}{|U_{std-db}^2 + U_{db}^2|}\frac{(V_{cb}^* V_{cs})}{(V_{cb}^* V_{cs})^*}\right]$$

- $B_d^0 \to \pi^+\pi^-$

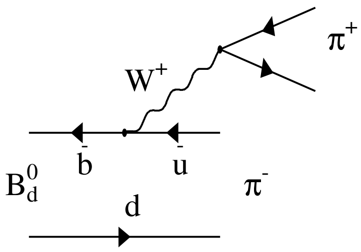

$$\sin(2\alpha) \equiv -A_{B_d^0 \to \pi^+\pi^-} = -\mathrm{Im}\left[\frac{(U_{std-db}^2 + U_{db}^2)}{|U_{std-db}^2 + U_{db}^2|}\frac{(V_{ub}^* V_{ud})}{(V_{ub}^* V_{ud})^*}\right]$$

9 CP Violation and $\sin(\gamma)$ in $\bar{b} \to \bar{u} + c + \bar{s}$

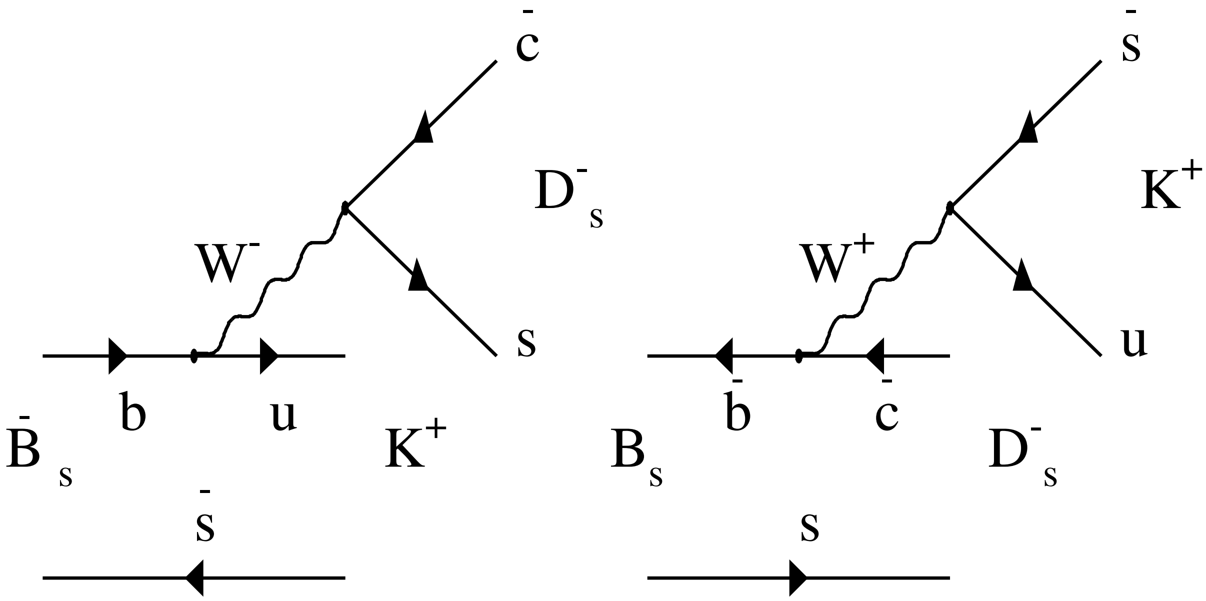

The B_s oscillation amplitude is almost real, allowing phases from decay amplitudes to be measured alone. The phase is

$$\phi_{qf} = -(2\phi(B_q \to \bar{B}_q) + \phi(\bar{B}_q \to f) - \phi(B_q \to f))$$

Two of the four processes, out of those for B_s and $\bar{B}_s$ decays into final states f and $\bar{f}$, must be measured together. The largest branching ratios for $\sin(\gamma)$ processes is in

$$B_s,\ \bar{B}_s \to D_s^{\pm}\ K^{\mp}$$

where the $BR \approx 2 \times 10^{-4}$

Here, the $\bar{B}_s$ decay to the final state involves V_{ub}^*, but the conjugate process for B_s does not involve $b \to u$ and is thus almost real. Since
$V_{ub} = s_{13}e^{-i\gamma}$, and B_s mixing is almost real, the final asymmetry which is the imaginary part, only involves $\sin(\gamma)$, not $\sin(2\gamma)$.

In the four down quark model

$$\sin(\gamma) = \mathrm{Im}\left(\frac{(U^2_{std-bs} + U^2_{bs})}{|U^2_{std-bs} + U^2_{bs}|}\frac{(V^*_{ub}V_{cs})}{|V_{ub}V_{cs}|}\right).$$

Since this imaginary part can be both positive and negative, we now include the full range $-1 \leq \sin(\gamma) \leq 1$ motivated by Wolfenstein's approach of finding the full range of predictions, rather than perturbations around the SM result.

10 The "Frequency" of B_s Oscillations, x_s

Here we exclude the theoretical uncertainty on $B_{B_s} f^2_{B_s}$, and take the ratio of x_s to x_d, which is better calculated, and in which we have also included the FCNC with Z^0 exchange

$$x_s = 1.35\ x_d \frac{|U^2_{std-bs} + U^2_{bs}|}{|U^2_{std-db} + U^2_{db}|}$$

We now include the amplitude method analysis of LEP with SLD to assign a $\Delta\chi^2$ for each x_s calculated in the parameter grid.

11 The B_s Decay Asymmetry, A_{B_s}

In the standard model, B_s mixing involves $(V^*_{ts}V_{tb})^2$ which is almost exactly real. Thus no CP violating phase develops in the most likely B_s decays involving the real amplitude for $\bar{b} \to \bar{c} + c + \bar{s}$. This occurs in the decays $B_s \to J/\Psi\phi$, $B_s \to D^+_s D^-_s$, and $B_s \to J/\Psi K_S$.

In the four down quark model, the CP violating decay asymmetry is

$$A_{B_s} = \mathrm{Im}\left(\frac{(U^2_{std-bs} + U^2_{bs})}{|U^2_{std-bs} + U^2_{bs}|}\frac{(V^*_{cb}V_{cs})}{(V_{cb}V^*_{cs})}\right).$$

Since this is an imaginary part of an $e^{i\Phi}$, we again include the full range $-1 \leq A_{B_s} \leq 1$.

12 Comprehensive Maximum Likelihood Analysis: Experiments and Degrees of Freedom

Standard Model

4 parameters (3 angles, 1 phase)

- 9 present experiments $\rightarrow$ 5 degrees of freedom
- B factory, add 2 expts. $\rightarrow$ 7 degrees of freedom

Four Down Quark Model

9 parameters (6 angles, 3 phases)

- 13 present experiments $\rightarrow$ 4 degrees of freedom
- B factory, add 2 expts. $\rightarrow$ 6 degrees of freedom

13 Standard Model $(\sin(2\alpha), \sin(2\beta))$ Plot - Present Constraints

- Present Data: $\sin(2\beta) \approx 0.65 \pm 0.15$.
- $\sin(2\alpha)$ unconstrained but not likely to be -1 or $+1$.

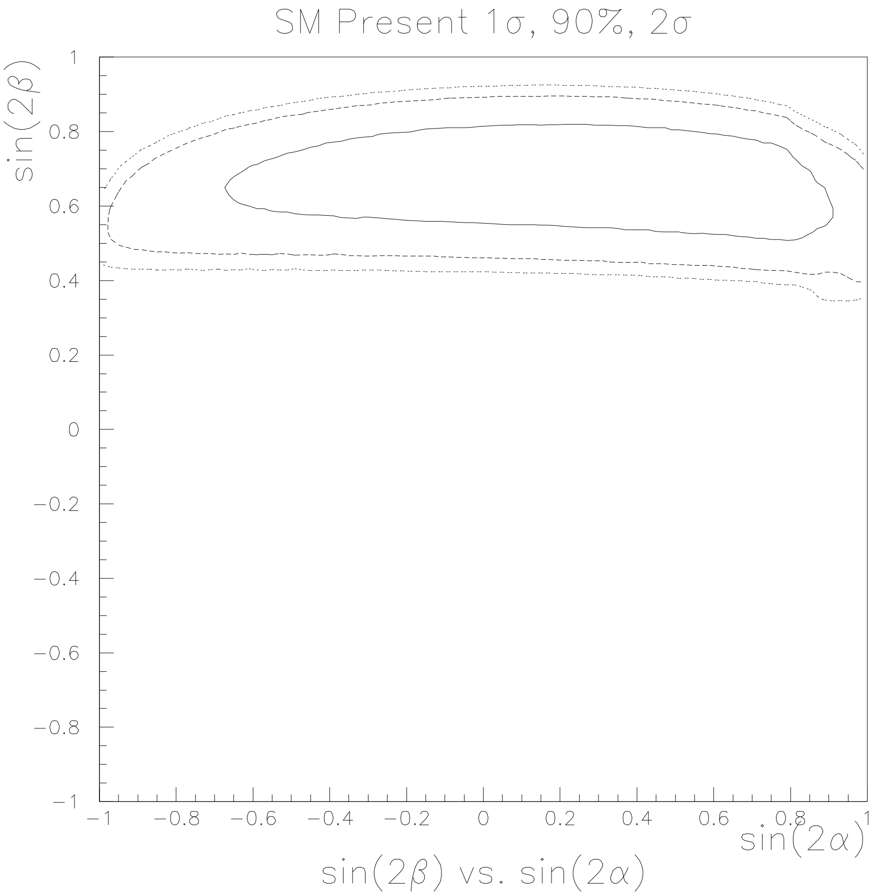

14 Four Down Quark Model $(\sin(2\alpha), \sin(2\beta))$ Plots - Present Limits

- ➤ The entire plane is allowed at 1-σ.
- ➤ Even a rough, early measurement of $\sin(2\beta)$ might give a surprising result.

15 Standard Model (ρ, η) Plot (broad), with Projected B-Factory Cases (small)

- Contours are 1-σ (solid), 2-σ (dashed), and 3-σ (dotted).
- Cases of B factory results at $\sin(2\alpha) = 1, \quad 0, \quad -1$ are shown from left to right, respectively.

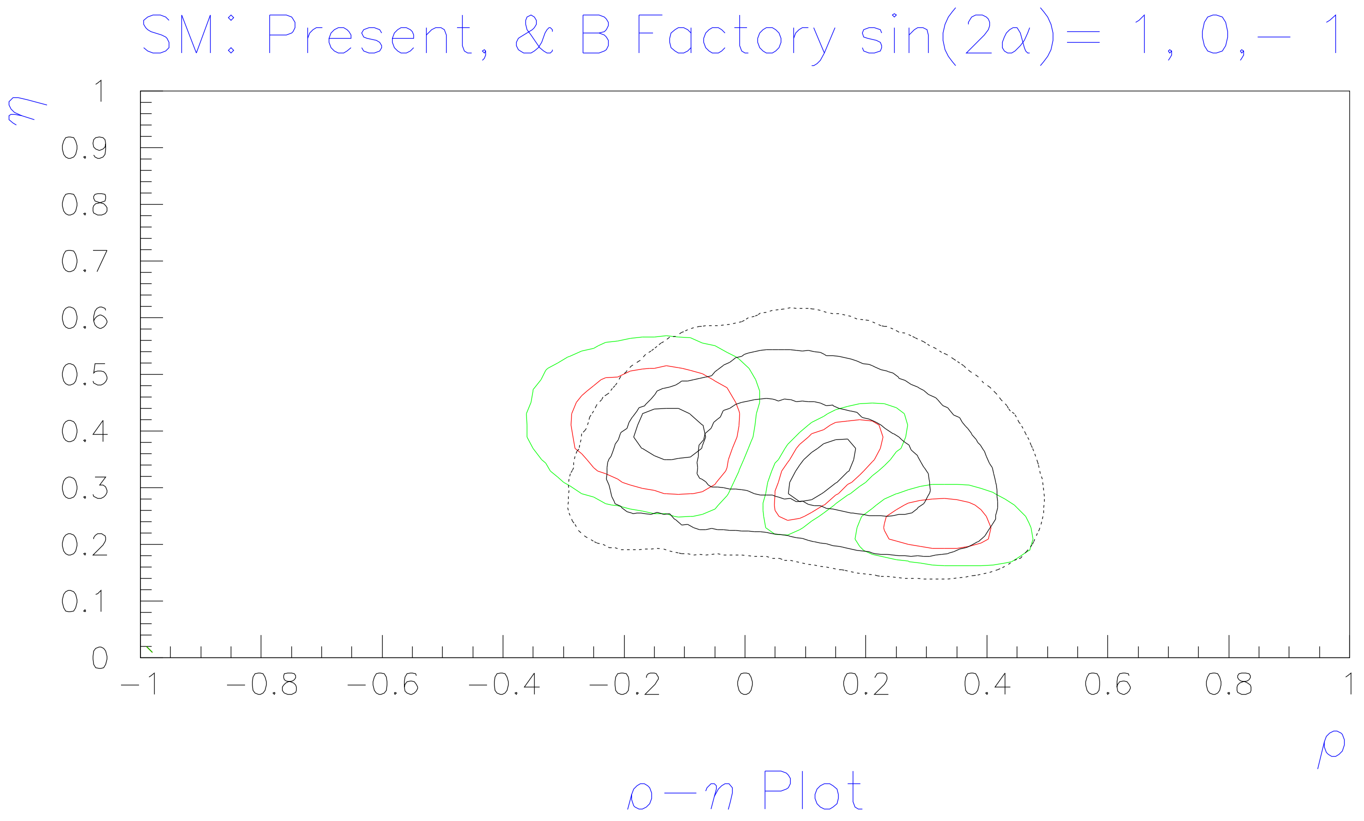

16 Four Down Quark Model: (ρ, η) Plots

- Here, the plotted ρ and η are taken as the coordinates of V_{ub}^*

$$\rho + i\eta = V_{ub}^*/|V_{cd}V_{cb}|$$

- The plots are extended to negative $\eta = \mathrm{Im}(V_{ub}^*/|V_{cd}V_{cb}|)$.
- There is now a unitarity quadrangle

$$V_{ub}^*V_{ud} + V_{cb}^*V_{cd} + V_{tb}^*V_{td} + V_{4b}^*V_{4d} = 0$$

  where the last term has limits $|U_{bd}/V_{cb}^*V_{cd}| \leq 0.1$.
- The circles in $\delta = \delta_{13}$ ($V_{ub}^* = s_{13}e^{i\delta_{13}}$) are due to δ_{14} or δ_{24} being the source of the observed CP violation in ϵ, so that δ_{13} is unconstrained.
- The multiple regions are now extended into the full (ρ, η) plane.

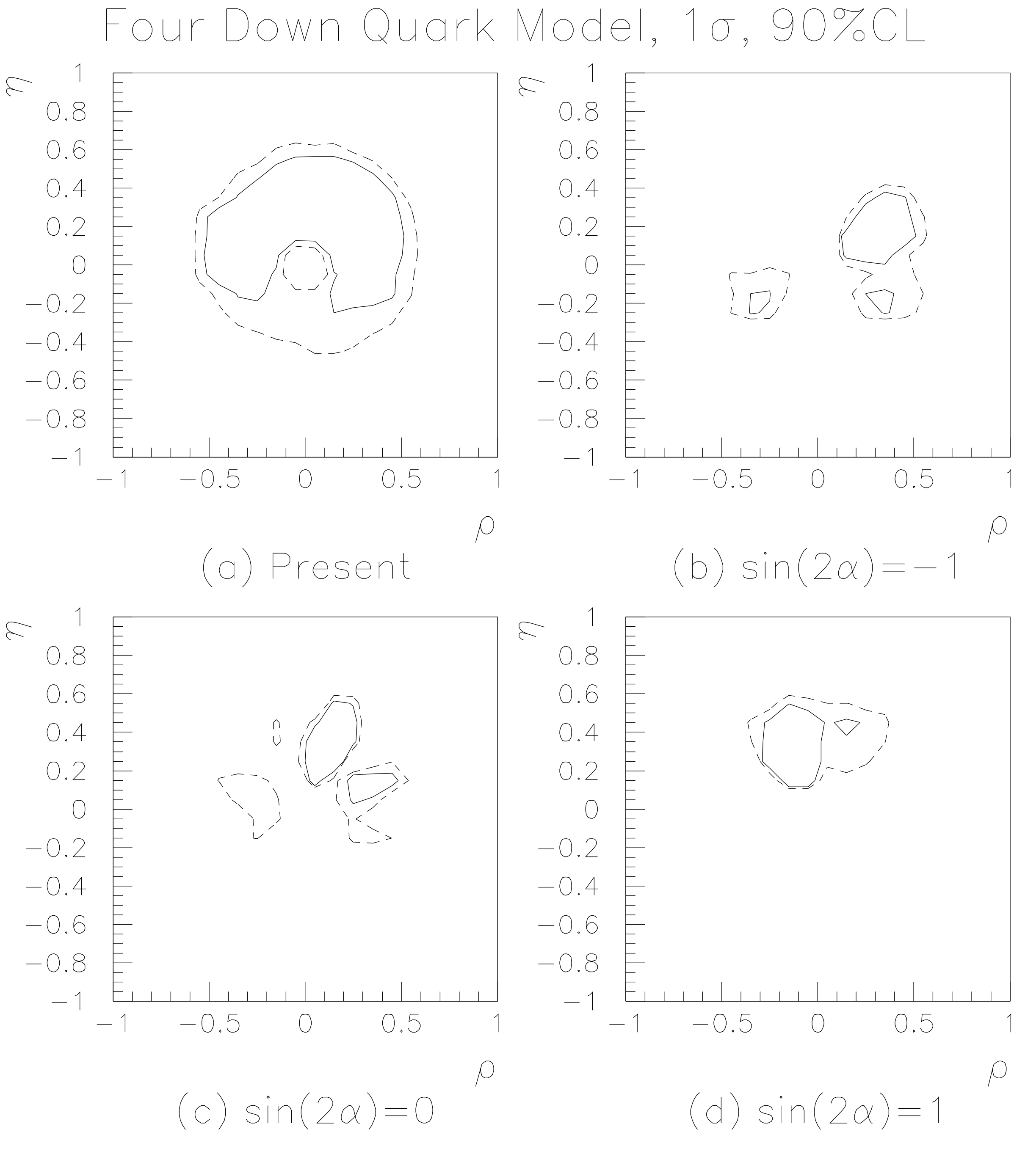
Four Down Quark Model, 1σ, 90%CL
η
1
0.8
0.6
0.4
0.2
0
−0.2
−0.4
−0.6
−0.8
−1
−1
−0.5
0
0.5
1
ρ
(a) Present
(b) sin(2α)=−1
(c) sin(2α)=0
(d) sin(2α)=1

17 Standard Model $(x_s, \sin(\gamma))$ Plots

- Present Data: $0.75 \leq \sin(\gamma) \leq 1, \quad 14 \leq x_s \leq 29$ at 1-σ.
- x_s measurement can strongly constrain $\sin(2\alpha)$.

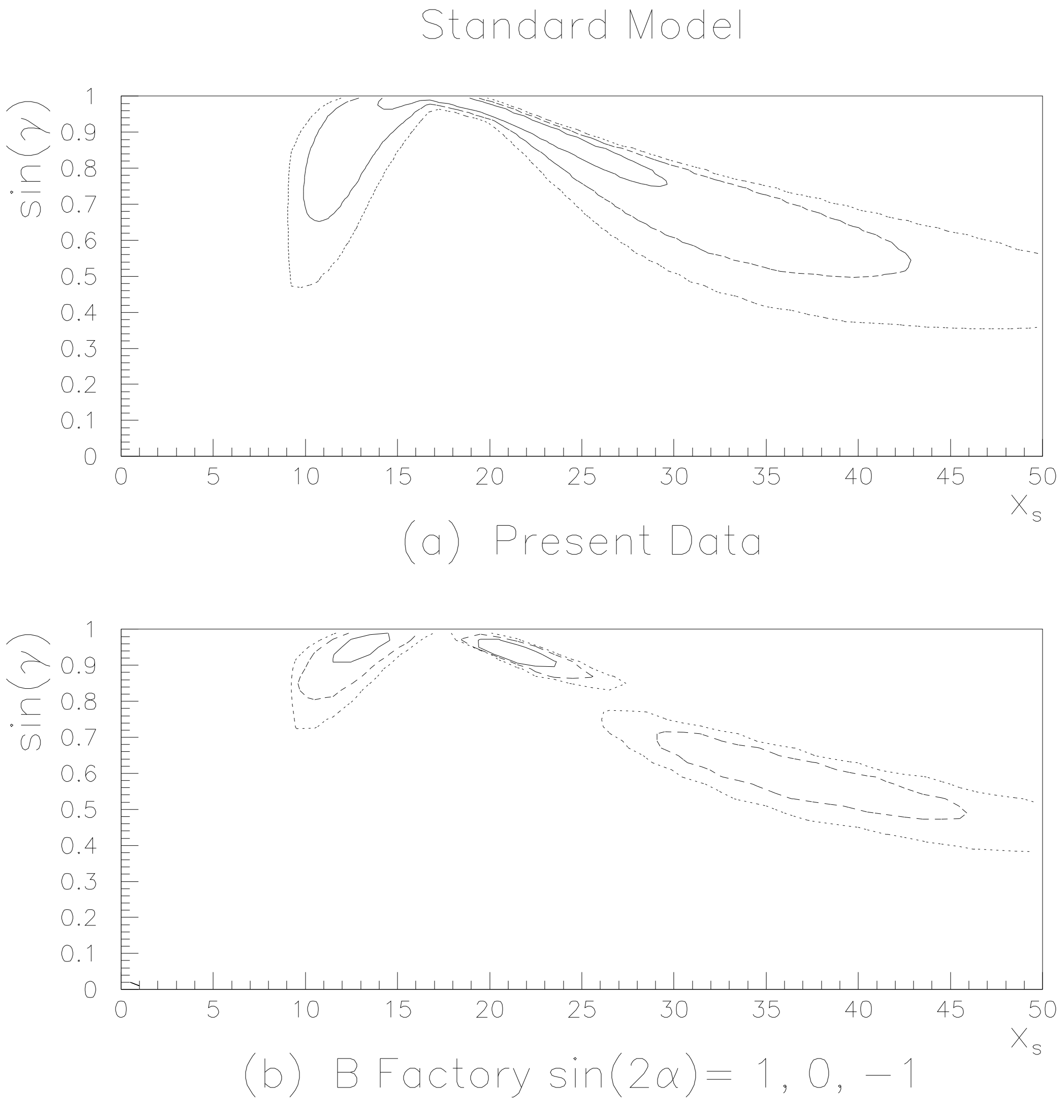

18 Four Down Quark Model $(x_s, \sin(\gamma))$ Plots

- Extended $\sin(\gamma)$ range to $-1 \leq \sin(\gamma) \leq 1$ for completeness.
- All $\sin(\gamma)$ is allowed at 1-σ, as opposed to the limited standard model range.
- The x_s allowed region is 12 to 50 at 1-σ, larger than in the standard model.

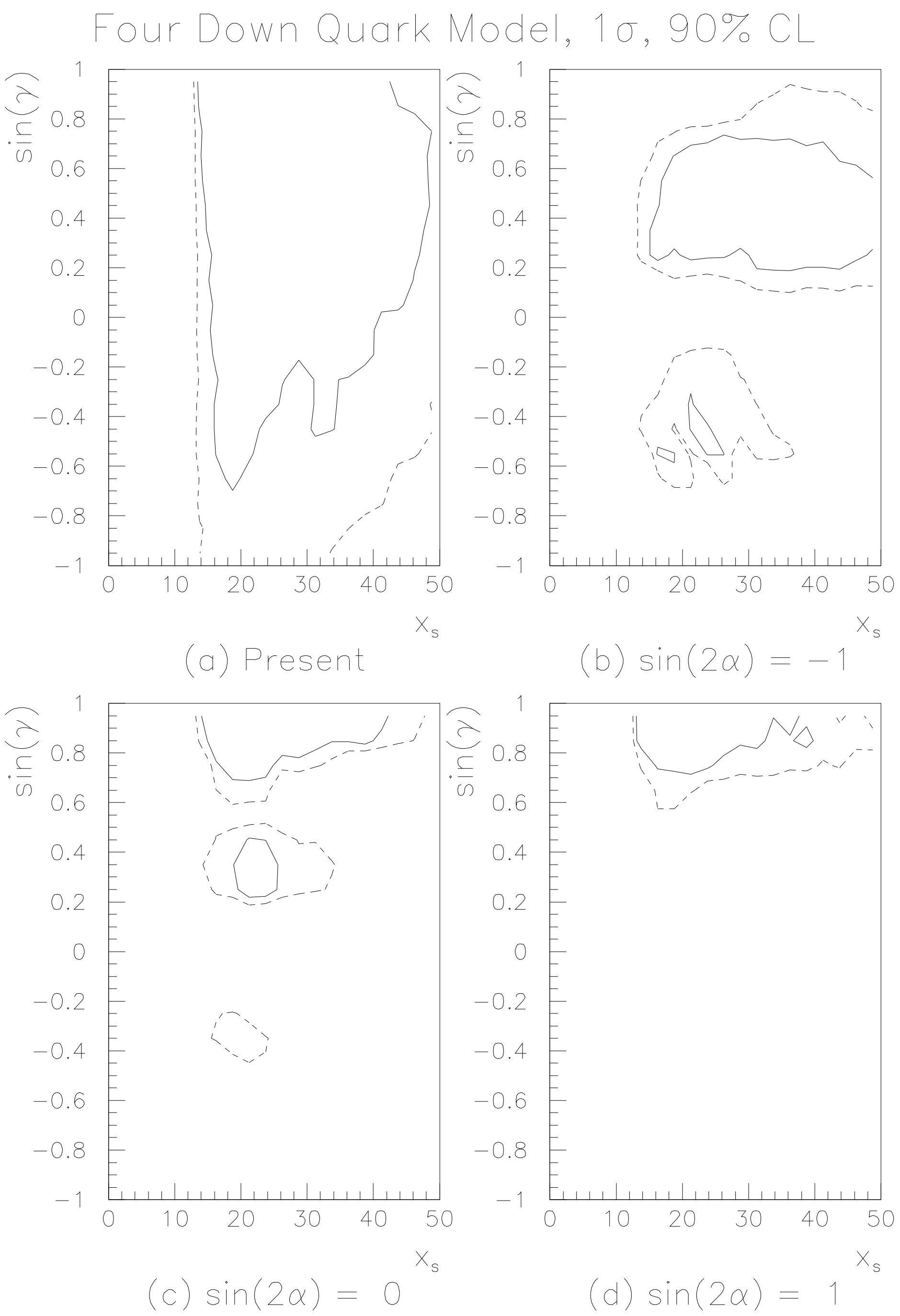

19 B_s Decay Asymmetry from B_s Mixing, A_{B_s}

- This is almost zero in the Standard Model, i.e. ≤ 0.025.
- $A_{B_s} = \mathrm{Im}(e^{i\Phi})$ is extended here to negative values, and appears roughly symmetric about 0.
- $|A_{B_s}| \leq 0.4$ at 1-σ is possibly detectable in the four down quark model.

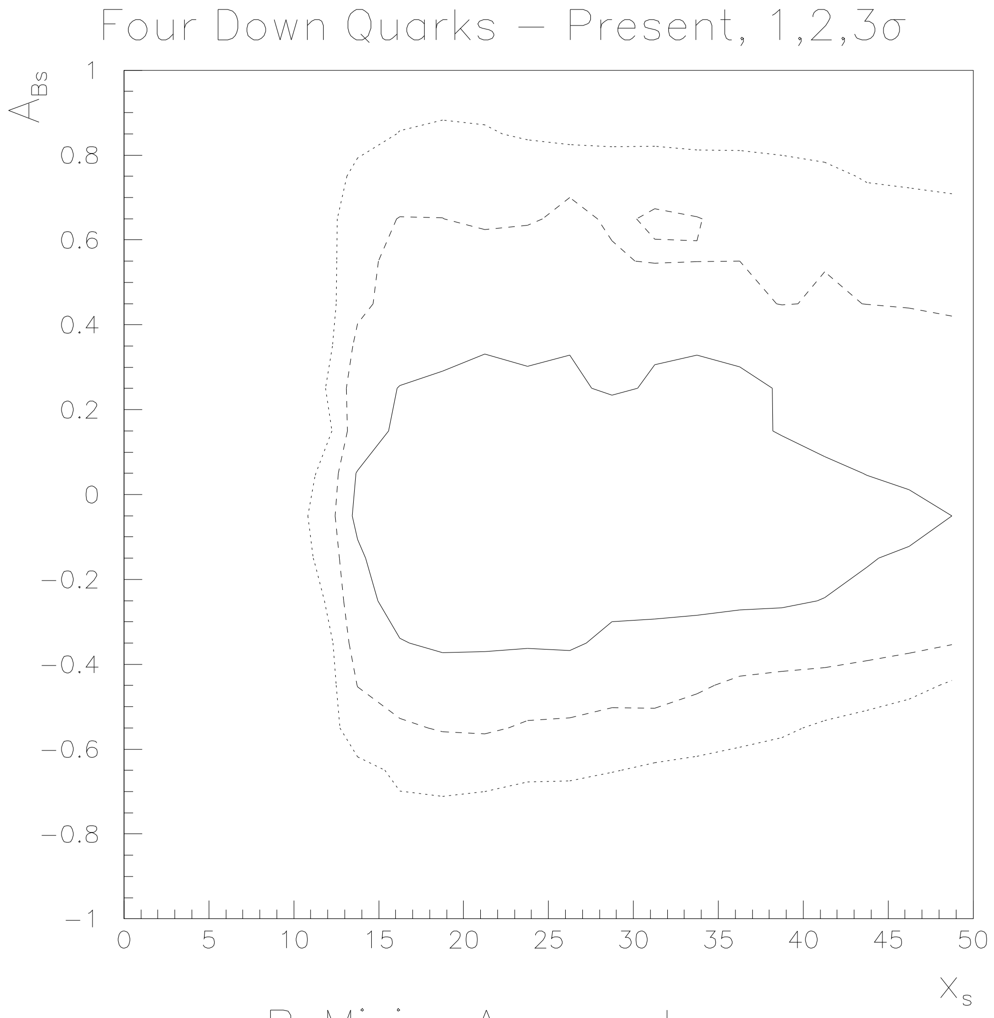

B_s Mixing Asymmetry vs x_s

20 Conclusions for Iso-singlet Down Quark Models

- FCNC can contribute significantly to $B_d - \bar{B}_d$ mixing and to $B_s - \bar{B}_s$ mixing, and give new phases.
- Since all $\sin(2\beta)$ and $\sin(2\alpha)$ are allowed, even an **early measurement** of $\sin(2\beta)$ will be significant and may be surprising.
- There are **multiple allowed regions** in the (ρ, η) and in the $(x_s, \sin(\gamma))$ plots from new physics with new phases after the B factory results.
- This will **require the additional experiments of x_s and $\sin(\gamma)$**, first to isolate a region, and then to rule in or out a new physics model.
- In new physics models, the SM phase **δ can be smaller or arbitrary**, with the other phases causing the presently observed CP violation.
- The present range for x_s is from 14 to 29 at 1-σ in the SM, and from 12 to 50 at 1-σ in the four down quark model.
- The $\sin(\gamma)$ range is from 0.75 to 1.0 in the SM, and **unrestricted at 1-σ** in the four down quark model.
- The **B_s CP violating decay asymmetry** is almost null in the SM, but could be as large in magnitude as ± 0.4 at 1-σ in the four down quark model.
- The **mass** of the lightest singlet down quark in E_6 could be roughly related to the mixing angle by

$$\begin{aligned} \theta_{34}^2 &\simeq m_b/m_D, \quad |V_{4b}| \simeq \theta_{34} \leq 0.06, \quad \text{giving} \\ m_D &\geq 250 \times m_b = 1.2 \text{ TeV}. \end{aligned}$$

21 Limiting regions of parameter space in $SU(2)_L \times SU(2)_R \times U(1)_{B-L}$

$SU(2)_R$ has two heavy charged $W_R^{\pm}$ and a Z_0'.

The charged weak current is

$$
\begin{aligned}
L &= \frac{g}{\sqrt{2}}(\bar{u}_L\gamma_\mu d_L + \bar{\nu}_L\gamma_\mu e_L)W_L^+ \\
&\quad + \frac{g}{\sqrt{2}}(\bar{u}_R\gamma_\mu d_R + \bar{\nu}_R\gamma_\mu e_R)W_R^+ + g^2\kappa\kappa' W_L^- W_R^+ + \text{H.C.}
\end{aligned}
$$

The lefthanded quark mixing matrix V^L is that of the standard model.

Langacker and Sankar have made a detailed analysis on W_R mass limits, and conclude that the lower limit of the W_R mass of 1.6 TeV for $V^L = V^R$ can be reduced by taking either of the following forms of V^R

$$V^R_{B_s} = \begin{array}{c} \\ u \\ c \\ t \end{array} \begin{array}{c} \begin{array}{ccc} d & s & b \end{array} \\ \begin{pmatrix} 1 & 0 & 0 \\ 0 & ce^{i\xi} & se^{i\sigma} \\ 0 & se^{i\phi} & ce^{i\chi} \end{pmatrix} \end{array}, \quad (\text{Case } B_s),$$

or

$$V^R_{B_d} = \begin{array}{c} \\ u \\ c \\ t \end{array} \begin{array}{c} \begin{array}{ccc} d & s & b \end{array} \\ \begin{pmatrix} 0 & 1 & 0 \\ ce^{i\xi} & 0 & se^{i\sigma} \\ se^{i\phi} & 0 & ce^{i\chi} \end{pmatrix} \end{array}, \quad (\text{Case } B_d).$$

Here $s = \sin\theta$ and $c = \cos\theta$ $(0 \le \theta \le 90^\circ)$, and the unitarity condition is

$$\xi - \sigma = \phi - \chi + \pi.$$

These regions of parameter space work because they introduce zeroes for couplings of W_R to c and t quarks from either d quarks (Case B_s) or s quarks (Case B_d).

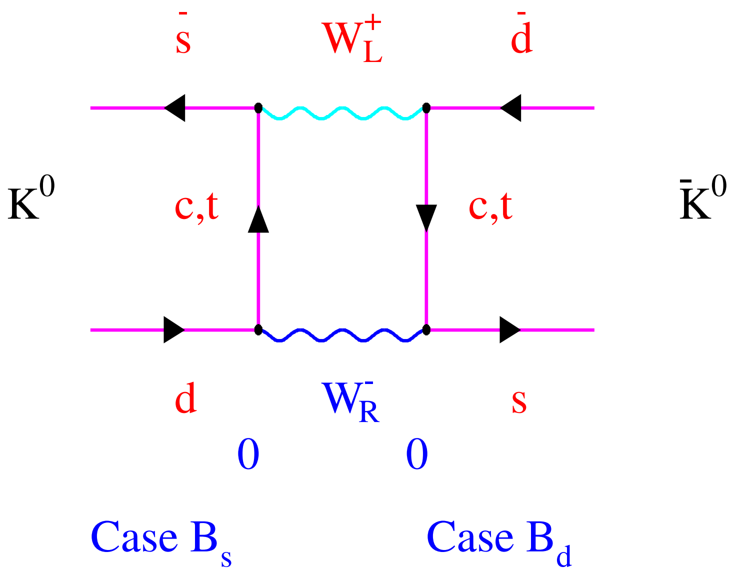

22 CP Violation in K Mesons in the LRSM

$$\epsilon_K \approx \mathrm{Im} < K^0|H(\Delta S = 2)|\bar{K}^0 > /\sqrt{2}\Delta m_K$$

where $H(\Delta S = 2)$ is the Hamiltonian from the box diagrams mediated by two W_L, two W_R, or a W_L-W_R pair.

The H^{LL} contribution is

$$\epsilon_K = \frac{G_F^2 f_K^2 B_K m_K m_W^2}{12\sqrt{2}\pi^2 \Delta m_K}[\eta_{cc} S(x_c) I_{cc} + \eta_{tt} S(x_t) I_{tt} + 2\eta_{ct} S(x_c, x_t) I_{ct}]$$

The two W_R part H^{RR} gives no contribution due to the factors I_{ij} vanishing for both cases of V^R.

The H^{LR} contribution is

$$\begin{aligned} H^{LR} &= \frac{2G_F^2}{\pi^2} m_{W_L}^2 \beta \sum_{i,j=u,c,t} \lambda_i^{LR} \lambda_j^{RL} (\bar{d}_R s_L)(\bar{d}_L s_R) \frac{\sqrt{x_i x_j}}{4} \\ &\quad [(4\eta_{ij}^{(1)} + \eta_{ij}^{(2)} x_i x_j \beta) I_1(x_i, x_j, \beta) - (\eta_{ij}^{(3)} + \eta_{ij}^{(4)} \beta) I_2(x_i, x_j, \beta)], \end{aligned}$$

where $\lambda_i^{LR} = V_{id}^{L*} V_{is}^R$, $\beta = (m_{W_L}/m_{W_R})^2$, and $x_i = m_i^2/m_{W_L}^2$.

The contribution to ϵ_K from H^{LR} only comes from the surviving terms on $\lambda_i^{LR} \lambda j^{RL}$.

The contribution to ϵ_K from H^{LR} only comes from the surviving terms on $\lambda_i^{LR}\lambda j^{RL}$:

$$\begin{array}{lll} \text{Case } B_s & (\text{cu pair}): & \lambda^2 c \sin(-\xi) \\ & (\text{tu pair}): & A\lambda^4[(1-\rho)\sin(\phi) + \eta\cos(\phi)]. \end{array}$$

$$\begin{array}{lll} \text{Case } B_d & (\text{uc pair}): & (1-\lambda^2/2)^2 c \sin(-\xi) \\ & (\text{ut pair}): & As\lambda^2(1-\lambda^2/2)\sin(-\phi). \end{array}$$

Limiting parameters:

Due to the smallness of $\epsilon_K = (2.28 \pm 0.02) \times 10^{-3}$, one adjusts the parameters in V^R so that no contribution to ϵ_K will come from H^{LR}.

$$\begin{array}{lll} \text{Case } B_s: & \sin(\xi) = 0, & \tan(-\phi) = \dfrac{\eta}{(1-\rho)}. \\ \text{Case } B_d: & c = 0, \quad (V_{tb}^R = 0) & \sin(\phi) = 0. \end{array}$$

Case B_s:

Two new parameters in $V^R_{B_s}$: θ ($s = \sin\theta$) and σ, with $\phi = -\beta$, $\xi = 0$, and $\chi = \pi + \sigma - \beta$, where β is the angle of the unitarity triangle at the (ρ, η) point being explored.

$$V^R_{B_s} = \begin{array}{c} \\ u \\ c \\ t \end{array} \!\!\begin{array}{c} \begin{array}{ccc} d & s & b \end{array} \\ \begin{pmatrix} 1 & 0 & 0 \\ 0 & c & se^{i\sigma} \\ 0 & se^{-i\beta} & -ce^{i(\sigma-\beta)} \end{pmatrix} \end{array}.$$

Case B_d:

One new parameter in $V^R_{B_d}$: σ, giving

$$V^R_{B_d} = \begin{array}{c} \\ u \\ c \\ t \end{array} \!\!\begin{array}{c} \begin{array}{ccc} d & s & b \end{array} \\ \begin{pmatrix} 0 & 1 & 0 \\ 0 & 0 & e^{i\sigma} \\ 1 & 0 & 0 \end{pmatrix} \end{array}.$$

23 $B^0 - \bar{B}^0$ Mixing

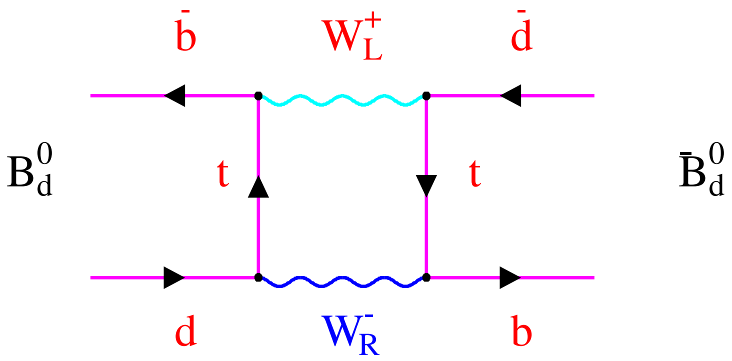

$$M_{12} = M_{12}^{LL} + M_{12}^{RR} + M_{12}^{LR},$$

corresponding to the contributions from box diagrams in which two W_L, two W_R and a W_L-W_R pair are exchanged.

$$\begin{aligned} M_{12}^{RR} &= \frac{G_F^2}{12\pi^2} m_B m_{W_L}^2 (f_B^2 B_B)\eta_{tt} S(x_t)\beta^2 (V_{tq}^{R*} V_{tb}^R)^2. \\ &= 0 \ \text{ in } B_d; \qquad \neq 0 \text{ in } B_s. \end{aligned}$$

$$\begin{aligned} M_{12}^{LR} &= \frac{G_F^2}{2\pi^2} m_B (f_B^2 B_B)(\frac{m_B}{m_b})^2 m_{W_L}^2 \beta \sum_{i,j=u,c,t} \lambda_i^{LR} \lambda_j^{RL} \frac{\sqrt{x_i x_j}}{4} \\ & [(4\eta_{ij}^{(1)} + \eta_{ij}^{(2)} x_i x_j \beta) I_1(x_i, x_j, \beta) - (\eta_{ij}^{(3)} + \eta_{ij}^{(4)} \beta) I_2(x_i, x_j, \beta)], \end{aligned}$$

where $\lambda_i^{LR} = V_{iq}^{L*} V_{ib}^R$ and $\lambda_i^{RL} = V_{iq}^{R*} V_{ib}^L$.

Dominant terms in the sum, quoted below, are largely determined by the quark mass factors $\sqrt{x_i x_j} = m_i m_j / m_{W_L}^2$.

$$(t,t) = 11.9, \ \ (t,c) = 4.6 \times 10^{-2}, \ \ \text{the rest } < \ 10^{-3}$$
$$(c,t) = 5.0 \times 10^{-2}, \ \ (u,t) = 0.8 \times 10^{-2}$$

24 Numerical Results for $B_d - \bar{B}_d$ Mixing

Case	Comparison with SM	W_R effect
B_s	$M_{12}^{LR} \ll M_{12}^{LL}$	No
B_d	$M_{12}^{LR} \sim M_{12}^{LL}$ $(M_{W_R} = 5\ \mathrm{TeV})$	Yes (c, t)
	$M_{12}^{LR} \leq 10^{-2} M_{12}^{LL}$ $(M_{W_R} = 10\ \mathrm{TeV})$	No

25 Numerical Results for $B_s - \bar{B}_s$ Mixing

Case	Comparison with SM	W_R effect
B_s	$M_{12}^{LR} \sim M_{12}^{LL}$ $(M_{W_R} = 5\ \mathrm{TeV})$	Yes (t, t)
	$M_{12}^{LR} \ll M_{12}^{LL}$ $(M_{W_R} = 10\ \mathrm{TeV})$	No
B_d	$M_{12}^{LR} \ll M_{12}^{LL}$	No

26 χ^2 Plots for (ρ, η), $(\sin(2\alpha), \sin(2\beta))$, and $(x_s, \sin(\gamma))$ in the LRSM

- **CKM Experiments (5) for SM - Present Data**
  - **Charged Current: (λ fixed)**

$$\begin{aligned} |V_{cb}| &= 0.039 \pm 0.004 \\ |V_{ub}/V_{cb}| &= 0.080 \pm 0.016 \quad \text{(CLEO II)} \end{aligned}$$

  - **Neutral Current:**

x_d

$|\epsilon|$

x_s bounds

- ***B* Factory Experiments (2):**

sin (2β)

sin (2α)

- **Left Right Symmetric Model:** (for various choices of W_R)

  With B factory experiments included, we have 5 + 2 = 7 experiments.

  Case B_s: 5 parameters (3 angles and 2 phases), or 2 degrees of freedom

  Case B_d: 4 parameters (2 angles and 2 phases), or 3 degrees of freedom.

Experimental results predicted with M_{12} including the LRSM

$$\sin(2\beta) \equiv \text{Im}\left(\frac{M_{12}^*}{|M_{12}|}\frac{V_{cb}^* V_{cs}}{V_{cb} V_{cs}^*}\right), \qquad \sin(2\alpha) \equiv \text{Im}\left(\frac{M_{12}^*}{|M_{12}|}\frac{V_{ub}^* V_{ud}}{V_{ub} V_{ud}^*}\right)$$

$$\sin(\gamma) \equiv \text{Im}\left(\frac{M_{12}^{B_s}}{|M_{12}^{B_s}|}\frac{V_{ub}^* V_{cs}}{|V_{ub} V_{cs}|}\right), \qquad x_s = 1.35 x_d \frac{|M_{12}^{B_s}|}{|M_{12}^{B}|}.$$

27 LRSM $(x_s, \sin(\gamma))$ Plots for Case B_s

- The entire $\sin(\gamma)$ range is allowed for the smaller W_R values.
- Larger x_s values are allowed for intermediate W_R values.

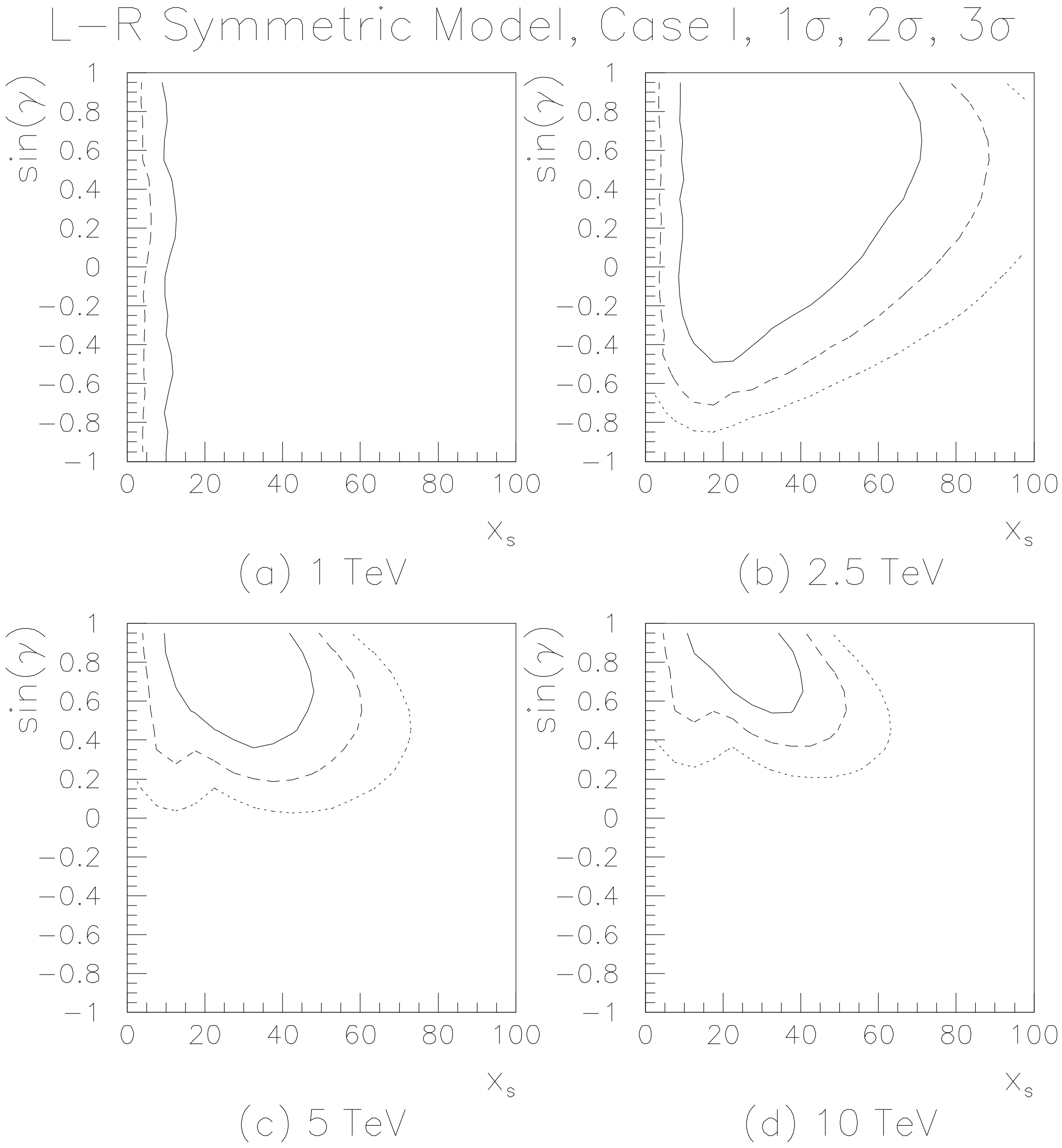

28 LRSM (ρ, η) Plots for Case B_d

➤ For M_{W_R} there are different or larger regions than in the SM.

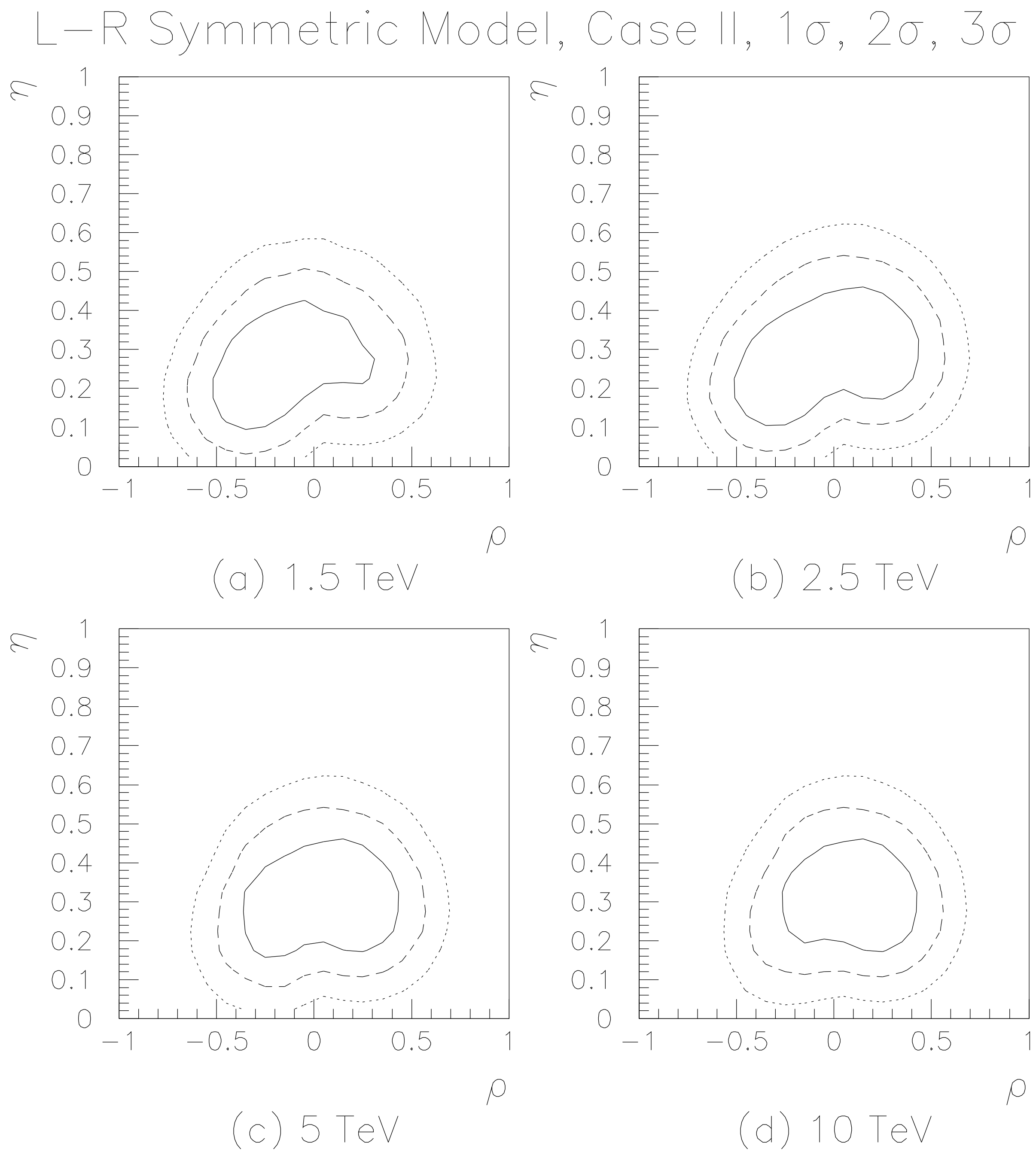

29 LRSM $(\sin(2\alpha), \sin(2\beta))$ Plots for Case B_d

➤ Different preferred 1-σ regions exist between $M_{W_R} = 1.5$ TeV and $M_{W_R} \geq 10$ TeV which is the SM region.

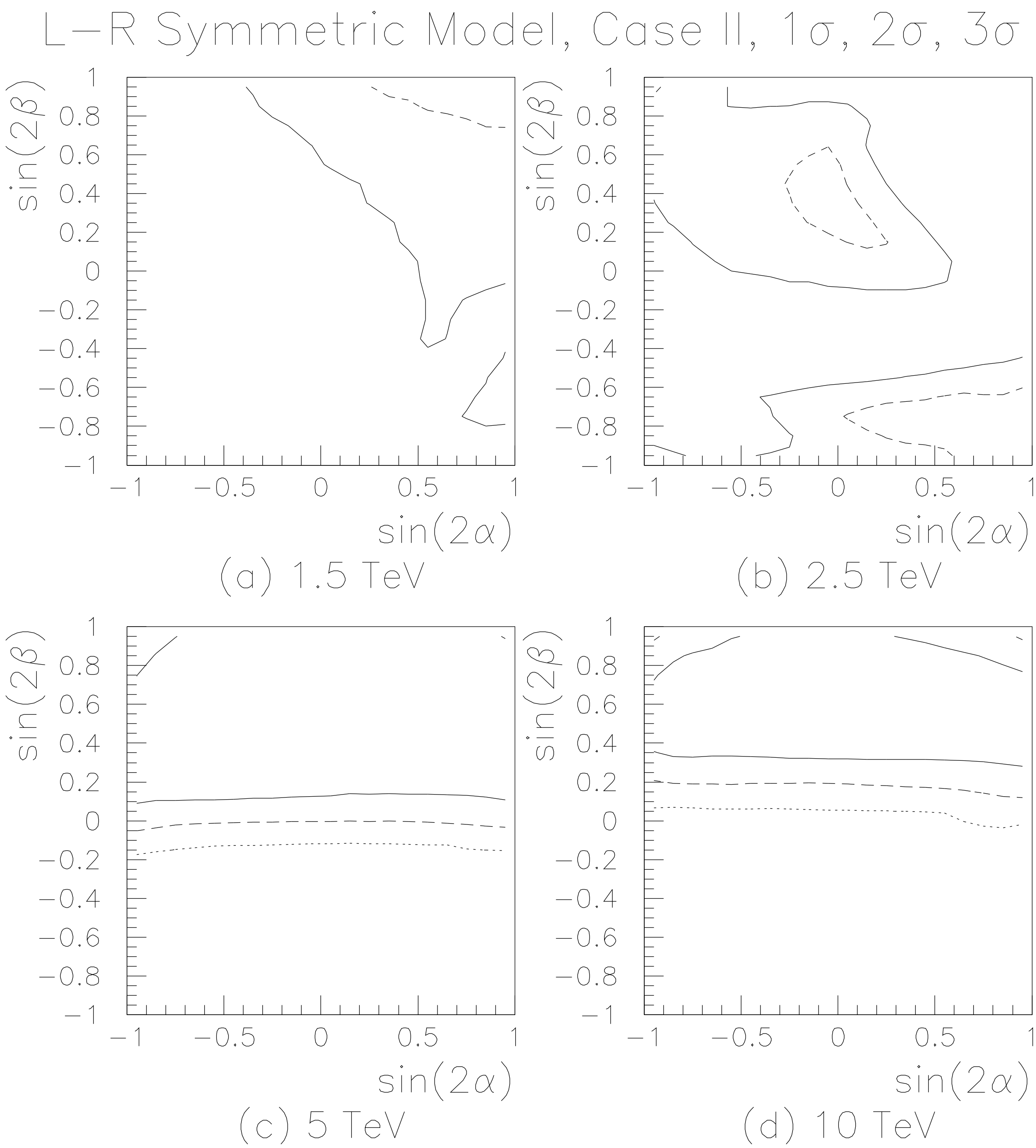

30 LRSM $(x_s, \sin(\gamma))$ Plots for Case B_d

➤ Lower $\sin(\gamma)$ is allowed than in the SM for $M_{W_R} \leq 2.5$ TeV.

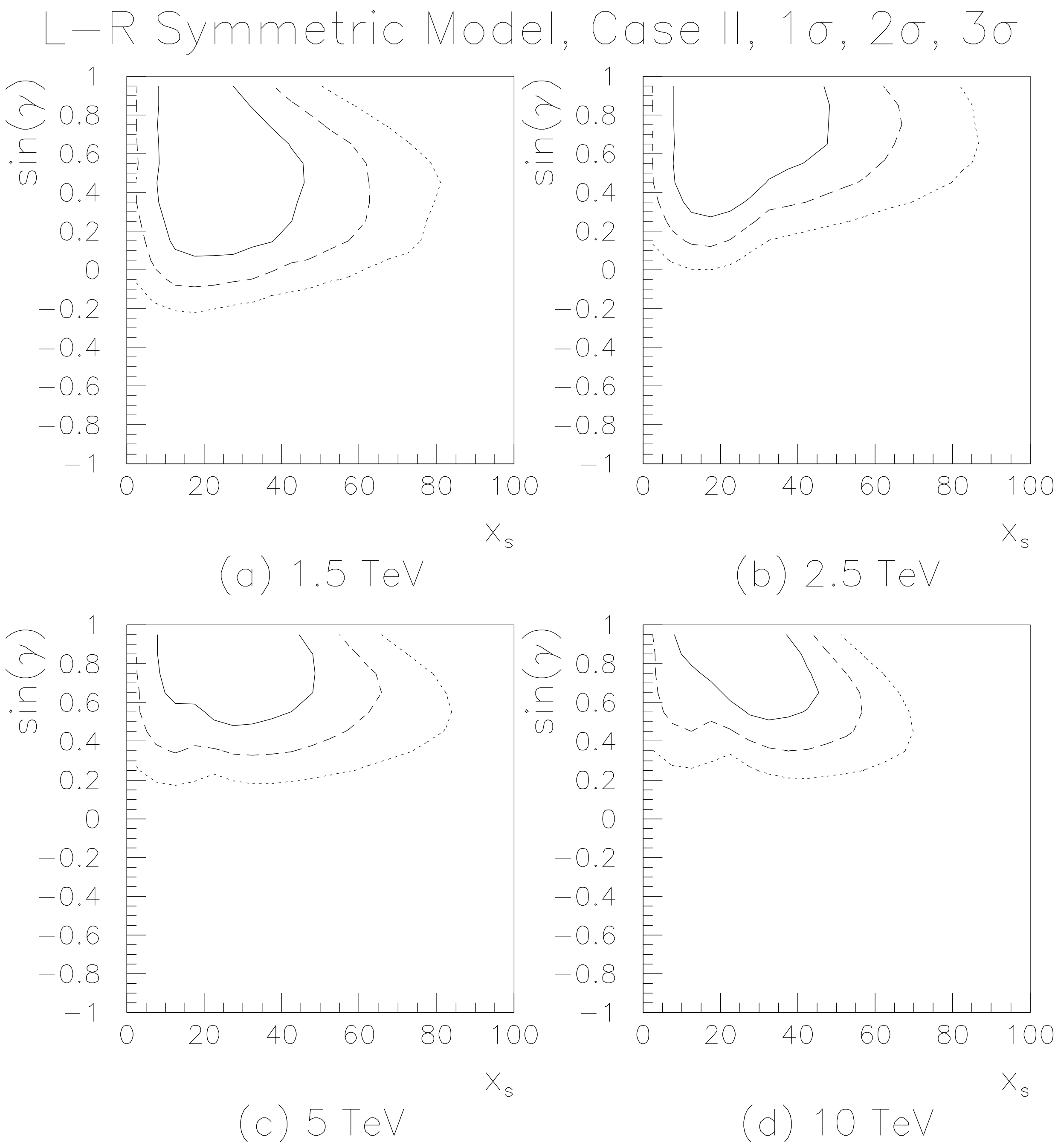

31 LRSM (x_s, A_{B_s}) Plots for Case B_s

- Whereas A_{B_s} is almost null in the SM, in the LRSM for $M_{W_R} \simeq 1$ TeV, this could saturate at $|A_{B_s}| \leq 1$. Even at larger $M_{W_R} \simeq 5$ TeV, this could be as large as 0.4.

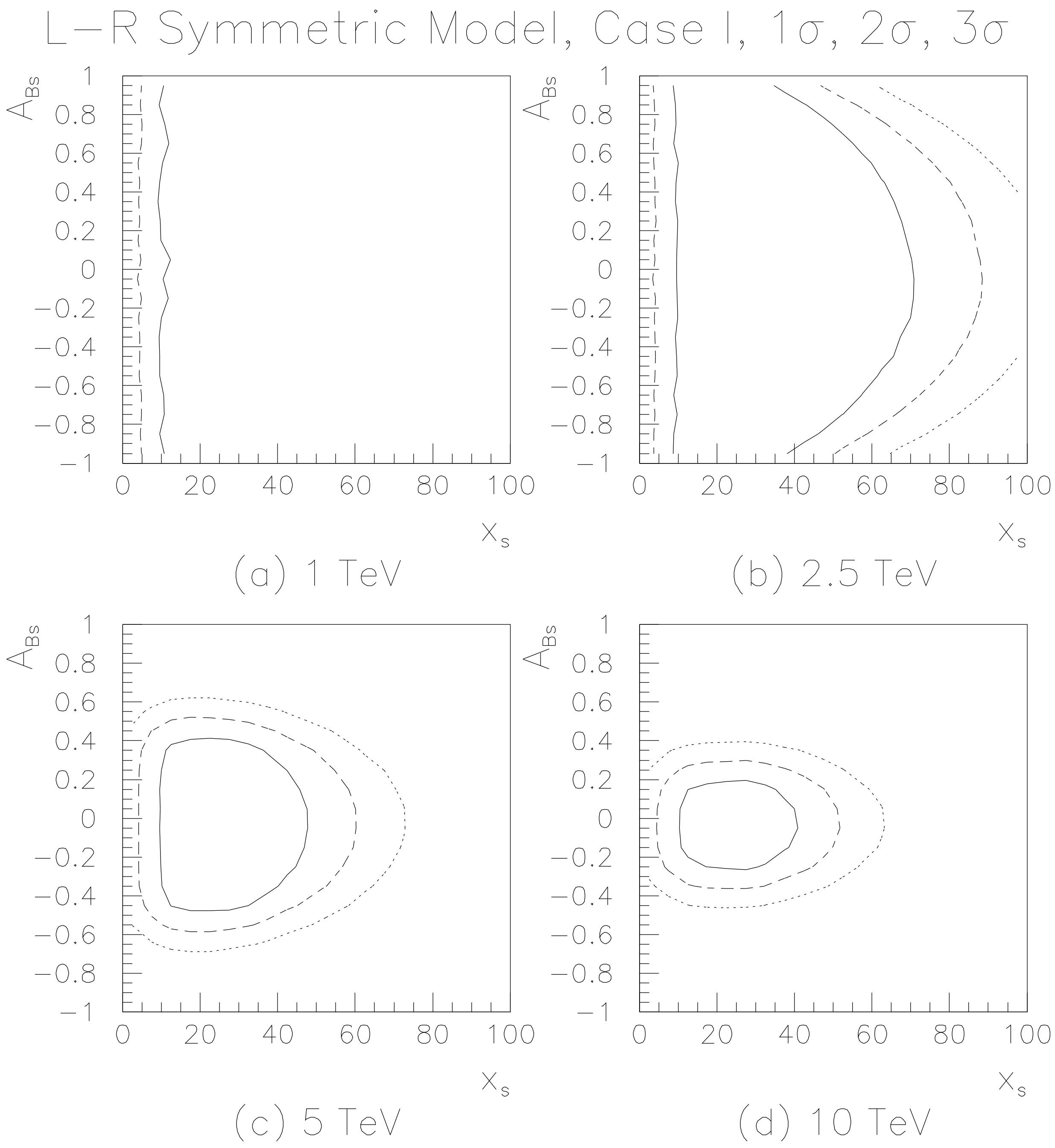

32 Conclusions for LRSM

- The LRSM can contribute significantly to $B_d - \bar{B}_d$ mixing (from case B_d) and to $B_s - \bar{B}_s$ mixing (from case B_s), and give new phases.
- W_R shows its effects in (ρ, η), in $(\sin(2\alpha), \sin(2\beta))$, and in $(x_s, \sin(\gamma))$ in case B_d, and in $(x_s, \sin(\gamma))$ in case B_s, both for $M_{W_R} \leq 5$ TeV.
- $\sin(2\beta) \simeq 0.65 \pm 0.15$, and $\sin(2\alpha)$ are only partly constrained in the SM. In the LRSM, all $\sin(2\beta)$ is allowed for $M_{W_R} \leq 2.5$ TeV.
- The present range for x_s is from 14 to 29 at 1-σ in the SM. The range in the LRSM is both lower and greater than that in the SM by about a factor of two, combining the two cases.
- The $\sin(\gamma)$ range is from 0.8 to 1.0 in the SM, and is largely unrestricted for case B_s in the LRSM for $M_{W_R} < 2.5$ TeV.
- The values for A_{B_s} could be very large and detectable in the LRSM.
- If the results from the B factory, x_s and $\sin(\gamma)$ are consistent with the SM, the current LRSM bound will increase from about $M_{W_R} \geq 0.8$ TeV (or 1.6 TeV with $V^R = V^L$) to $M_{W_R} \geq 5$ TeV.
- Even avoiding the ϵ_K constriant, the other experiments still require $M_{W_R} \geq 0.8$ TeV for a $1 - \sigma$ contour to exist in our plots.